12-1-2014

Molecular physics of elementary processes relevant to hypersonics: Electron-molecule collisions

R Celiberto
Istituto di Metodologie Inorganiche e Plasmi, CNR, Bari, Italy

V Laporta
University College London

A Laricchiuta
Istituto di Metodologie Inorganiche e Plasmi, CNR, Bari, Italy

J Tennyson
University College London

J. M. Wadehra
Wayne State University, ad5541@wayne.edu

The Open Plasma Physics Journal, 2014, *7*, (Suppl 1: M2) 33-47

Molecular Physics of Elementary Processes Relevant to Hypersonics: Electron-Molecule Collisions

R. Celiberto[*,1,2], V. Laporta[2,3], A. Laricchiuta[2], J. Tennyson[3] and J.M. Wadehra[4]

[1]*Dipartimento di Ingegneria Civile, Ambientale, del Territorio, Edile e di Chimica, Politecnico di Bari, Bari, Italy*

[2]*Istituto di Metodologie Inorganiche e Plasmi, CNR, 70125 Bari, Italy*

[3]*Department of Physics and Astronomy, University College London, London WC1E 6BT, UK*

[4]*Physics Department, Wayne State University, Detroit, MI 48202, USA*

Abstract: Non-resonant, electron-impact, vibro-electronic excitation cross sections, involving vibrationally excited N_2 molecules, to the mixed valence-Rydberg $b,c,o\ ^1\Pi_u$ and $b',c',e'\ ^1\Sigma_u^+$ singlet states are presented. These cross sections are calculated using the so-called *similarity approach*, accounting for the vibronic coupling among excited states, and compared with the experiments and different theoretical calculations.

New cross sections for the electron-impact resonant vibrational excitation of CO_2 molecule are calculated, for the symmetric stretching mode, as a function of the incident electron energy and for the transitions $(\upsilon_i,0,0)\rightarrow(\upsilon_f,0,0)$ with $\upsilon_i=0,1,2$ and for some selected value of υ_f in the interval $\upsilon_i\le\upsilon_f\le10$. A resonance potential curve and associated widths are calculated using the R-matrix method. Rate coefficients, calculated by assuming a Maxwellian electron energy distribution function, are also presented for the same $(\upsilon_i,0,0)\rightarrow(\upsilon_f,0,0)$ transitions.

Electron-impact cross sections and rate coefficients for resonant vibrational excitations involving the diatomic species N_2, NO, CO, O_2 and H_2, for multi-quantic and mono-quantic transitions, are reviewed along with the cross sections and rates for the process of the dissociative electron attachment to H_2 molecule, involving a Rydberg excited resonant state of the H_2^- ion.

Keywords: Dissociative attachment, non-resonant collisions, resonant-collisions, vibrational excitations.

1. INTRODUCTION

The presence of molecular species in gaseous systems gives rise to a large variety of collisional and radiative processes, which involve the internal degrees of freedom of the molecules. In non-equilibrium conditions, these processes play a role of fundamental importance in redistributing the energy, and while the rotational population, due to the quasi-continuum structure of the rotation levels, can be considered in many situations as thermalized, vibrational distributions can largely deviate from the equilibrium state, so that the collisional processes may involve highly-excited vibrational levels [1].

In low-temperatures plasmas, which can be characterized by a non-negligible molecular and electronic densities, the impact of electrons on vibrationally excited molecules may assume a role of paramount importance in affecting the plasma properties. With this in view, we roughly classify electron-molecule collisions in two categories represented by the *non-resonant* collisions, where only exchange of energy or momentum may occur, and which include vibrationally elastic and inelastic processes and ionization, and *resonant collisions*, where the incident electron can be momentarily captured by the target molecule with formation of a negative ion in a resonant state [2]. In this latter case, the resonant state is characterized by a finite lifetime and can either give rise to dissociative electron attachment (DEA), where the molecule can be broken in fragments, one of which carries the additional negative charge, or to the resonant vibrational excitation (RVE) occurring through emission of the extra electron back to the continuum, which usually leaves the molecule in a final excited vibrational level. Excited electronic states can also be involved in both the above resonant and non-resonant processes, so that combined vibro-electronic excitations become possible. In addition, when the excited levels fall in a vibrational continuum, molecular dissociation can also take place.

It is worth noting that this distinction in resonant and non-resonant collisions, is only conventional and refers to different scattering regimes where different approximations can be used in the theoretical calculations. In those collisions where the incident electron, at low energy, penetrates the molecular cloud, the formation of a resonance requires an accurate theoretical description of the scattering event, usually based on close-coupling methods. On the other hand,

*Address correspondence to this author at the Dipartimento di Ingegneria Civile, Ambientale, del Territorio, Edile e di Chimica, Politecnico di Bari, Bari, Italy; Tel: +39 080 596 3570;
Fax: +39 080 596 3611; E-mail: r.celiberto@poliba.it

1876-5343/14

for large collision energies, or also large impact parameters (distant collisions), the capture of the incident electron becomes improbable and the theoretical description of the scattering process can be strongly simplified. Hence, Born-like or semi-classical approximations can be applied.

A theoretical kinetic model of a non-equilibrium molecular plasma, aimed at a realistic and predictive description of the system, must take into account all the possible collisional and radiative processes involving both electrons as well as heavy particles in their ground or excited states [1]. This is usually implemented by resorting to the so-called state-to-state approach to plasma kinetic modeling, according to which each molecule, in a given internal quantum state, is considered as an independent chemical species [3]. This requires, in principle, the knowledge of the cross sections for all the scattering processes starting from each molecular quantum state accessible in the system. Examples of application of the state-to-state approach are provided, in space explorations, by the plasma arising during the re-entry conditions of space shuttles which, entering the atmosphere of a planet, are exposed to gas friction and their kinetic energy is then transferred to the internal motions of the atmospheric molecules, so that the level population assumes a non-equilibrium distribution [4].

In this article, which is part of a series of papers by our collaboration devoted to the study of planetary atmospheric molecules, we present electron-molecule cross sections for vibrationally excited molecules relevant for re-entry problems. In particular, we will discuss the cross sections for processes involving the N_2, O_2 and NO molecules, components of the Earth's atmosphere, CO and CO_2 important for Venus and Mars atmospheres, and H_2 which is the main component of the gaseous giant planets. The article is divided in two parts. In Part I we will focus on electron-impact non-resonant collisions leading to vibro-electronic excitation of diatomic nitrogen molecules. The cross sections are calculated for excitation to the $b,c,o\ ^1\Pi_u$ and $b',c',e'\ ^1\Sigma_u^+$ electronic states of the N_2 molecules. In Part II, we present new resonant cross section and rate coefficient calculations for vibrational excitations of the symmetric streching mode of the CO_2 molecule. We also briefly review cross sections and rate coefficients for the vibrational excitation and dissociative attachment for the diatomic molecules mentioned above [5-10]. In particular in Part I, section 2, we introduce the non-resonant electron-N_2 molecule excitation processes, and in section 3 and 4 we will illustrate the *similarity approach* for cross section calculations and discuss the obtained results respectively. In Part II, section 5, we will briefly outline the theory for resonant collisions, and in section 6 we will present the original results for CO_2 molecule. In section 7 cross sections and rates for diatomic molecules will be reviewed and, finally, in section 8 we will give our conclusions.

PART I: NON-RESONANT COLLISIONS

2. N_2 MOLECULE DISSOCIATION: EXTREME ULTRA-VIOLET SYSTEMS

Excitation to the lowest three electronic states of the $^1\Sigma$ and $^1\Pi$ spectroscopic series for N_2 system, being dipole-coupled to the ground state and representing the dominant contribution to the extreme ultraviolet spectrum of N_2 plasmas, has received considerable attention since the 1980s [11, 12]. These states, usually denoted as $b,c,o\ ^1\Pi_u$ and b', c', $e'\ ^1\Sigma_u^+$ exhibit a strong inter-state coupling, due to their mixed valence-Rydberg character, resulting in significant perturbation of vibronic bands. Moreover, the vibrational levels are strongly predissociated [13, 14], therefore vibronic excitation channels contribute to the formation of atoms electronically excited, affecting the atomic concentration in the gas phase.

Among the previous works on the subject, special mention should be made of the pioneering work by Ermler *et al.* [11], who computed *ab-initio* potential energy curves and transition dipole moments for the singlet terms of the N_2 spectrum, and the work of Stahel *et al.* [12], who considered for the first time the electronic coupling and provided a complete quantitative vibrational analysis. Spelsberg and Meyer [15] performed new *ab-initio* calculations, within a multi-reference configuration interaction (MRCI) frame-work, giving accurate potential energy curves of singlet terms, both in the adiabatic and diabatic representations, and also for the *R*-dependent coupling terms in the region of effective interaction, while recently Khakoo *et al.* and Malone *et al.* [16, 17] have investigated experimentally the electron-impact excitation of these states, deriving differential cross sections from energy-loss spectra. Finally, very recently Little and Tennyson [18] have calculated a comprehensive set of curves for both singlet and triplet states of N_2.

Here we present excitation cross sections for the processes

$$N_2(X\ ^1\Sigma_g^+,\upsilon'')+e^-\rightarrow N_2(^1\Sigma_u^+,\upsilon')+e^-, \quad (1)$$

$$N_2(X\ ^1\Sigma_g^+,\upsilon'')+e^-\rightarrow N_2(^1\Pi_u,\upsilon')+e^-, \quad (2)$$

obtained in the framework of the phenomenological *similarity approach*, as discussed in the next section, modified to include the effects of vibronic coupling.

3. THEORETICAL APPROACH

Electron-impact excitation to these states has been considered in different theoretical approaches. Vibrationally-resolved cross sections are also derived in ref. [19], where however the vibronic coupling was not accounted for. The main consequence of vibronic coupling is that different electronic terms of the same symmetry lose their identity and should be treated as a complex of states.

The treatment of the vibronic coupling entails the numerical solution of a system of coupled radial Schrödinger equations [20],

$$\left[\hat{I}T+\hat{V}^d(R)-\hat{I}E\right]\hat{\chi}^d(R)=0, \quad (3)$$

where $\hat{V}^d(R)$, depending on the internuclear distance R, is the symmetric interaction matrix, whose diagonal elements are represented by the diabatic potentials, while off-diagonal elements are the non-adiabatic coupling terms. The solution $\hat{\chi}^d(R)$ is a normalized vector of final-state radial wave

functions, having a mixed character and containing information about all the coupled a, b and c electronic states, *i.e.*

$$\hat{\chi}^d(R) \equiv \begin{pmatrix} \chi_a^d(R) \\ \chi_b^d(R) \\ \chi_c^d(R) \end{pmatrix}. \quad (4)$$

Equation (3) was solved using a numerical code for a system of coupled second-order differential equations, based on a second-order finite difference method [21], using the diabatic potentials and coupling terms calculated using an accurate MRCI approach in ref. [15].

The electron-impact induced vibronic transitions were calculated in the frame of the *similarity approach* [22], that allows a simplified expression for the state-to-state cross section, *i.e.*

$$\sigma_{\upsilon'\upsilon''} = \frac{2\pi e^4}{(\Delta E_{\upsilon'\upsilon''})^2} f_{\upsilon'\upsilon''} \phi(x), \quad (5)$$

where $\Delta E_{\upsilon'\upsilon''}$ is the transition energy, $f_{\upsilon'\upsilon''}$ is the oscillator strength for the vibronic transition, ϕ is the so-called *similarity function*, a universal function of the reduced incident electron energy $x = E / \Delta E_{\upsilon'\upsilon''}$, describing the collision dynamics,

$$\phi(x) = \frac{\ln[1 + a\sqrt{x-1}\,]}{x+b}, \quad (6)$$

whose parameters $a \sim 0.5$ and $b \sim 3.0$ have been optimized so as to fit experimental data for a large number of atomic and molecular systems [22]. Like in other semi-classical approaches, the state-to-state cross section of Eq. (5) is factorized as the product of the oscillator strength of the transition, containing information on the molecular target structure, and the universal function $\phi(x)$ of the reduced incident electron energy, describing the collision dynamics. The extension of the approach to the treatment of vibronic coupled states goes through the re-definition of the oscillator strength

$$f_{\upsilon'\upsilon''} = \frac{2}{3}\frac{g_e}{g_g} \Delta E_{\upsilon'\upsilon''} |\langle \chi_a^d | M_a^d(R) | \chi_{\text{ground}} \rangle + \langle \chi_b^d | M_b^d(R) | \chi_{\text{ground}} \rangle + \langle \chi_c^d | M_c^d(R) | \chi_{\text{ground}} \rangle|^2, \quad (7)$$

where g_e and g_g are the statistical weights of the excited and ground electronic terms respectively [23]. $\chi_{\text{ground}}(R)$ and $\chi^d_{a,b,c}(R)$ are the ground and excited state vibrational wave functions, and $M^d_{a,b,c}(R)$ are the transition dipole moments coupling the ground and the *a,b,c* excited electronic states. The diabatic transition dipole moments for the $^1\Sigma_g^+$ and $^1\Pi_u$ states were calculated in ref. [15].

The total cross section for excitation from the different vibrational levels, υ'', of the ground state, to the complex of the excited states results from the summation of state-resolved cross sections over the final vibrational levels

$$\sigma_{\upsilon''}(E) = \sum_{\upsilon'} \sigma_{\upsilon'\upsilon''}(E), \quad (8)$$

The summation runs over levels lying below the lowest dissociation limit. Above this threshold the continuum of the dissociating state is coupled to the bound levels of the other electronic terms in the complex, and the dissociation character of the cross section should be estimated.

4. VIBRONIC EXCITATION CROSS SECTIONS

Total vibronic excitation cross sections are derived for the transitions to the singlet terms of the nitrogen spectrum. In order to compare the present calculations with different theoretical results, obtained in an *independent-state* description, each term in the summation is multiplied by the vibrational-dependent quantity $P_a^{\upsilon'} = \langle \chi_a^d | \chi_a^d \rangle$, which weights the state-character of the vibrational wave function with respect to the three coupled terms. For example in the case of the $b\ ^1\Pi_u$ state one has,

$$\sigma^b_{\upsilon''}(E) = \sum_{\upsilon'} \sigma_{\upsilon'\upsilon''}(E) P_b^{\upsilon'} \quad (9)$$

Fig. (**1**) displays the total cross section for excitation to the $^1\Pi_u$ complex from the υ'' =0 level. The vibronic excitation to the b state dominates, while the contributions to the c and o states are considerably smaller. The comparison with theoretical results of ref. [19], obtained using the Gryzinski approach, is reported in Fig. (**1a**). Though a fairly good agreement in found for the b state, for the c and o states the similarity approach seems to give much lower cross sections. However it should be stressed that in the coupled frame the number of final vibrational levels included in the calculations is lowered with respect to the decoupled description. In fact, as already stressed above, high-lying c and o vibrational levels are actually coupled to the b -state continuum, thus contributing to the direct dissociation.

Integral excitation cross sections have been derived from recent accurate experimental differential total cross sections by Khakoo *et al.* [16], the angular integration being carried out under the assumption of constant $\sigma(\theta,E)$ for the low $[\theta < 3^\circ]$ and high $[\theta > 130^\circ]$ scattering angles. In comparing the experiments with the theoretical results, it should be considered that the spectral energy window explored in the measurements is 12-13.82 eV, thus collecting emission from a finite number of υ' levels, *i.e.* b [υ' 0-14], c [υ' 0-3] and o [υ' 0-3]; furthermore, in the experimental paper [16] the vibrational analysis was performed assigning the emission intensity in a decoupled frame, i.e. considering each transition belonging only to one member of the coupled system, while in the present theoretical approach vibrational levels have a mixed character, the weight of each member being represented by P. Accounting properly for both effects, and using a level-character $P_a^{\upsilon'}$ switching from 0 to 1, cross sections have been corrected and theoretical and experimental results in Fig. (**1b**) are thus found in good agreement.

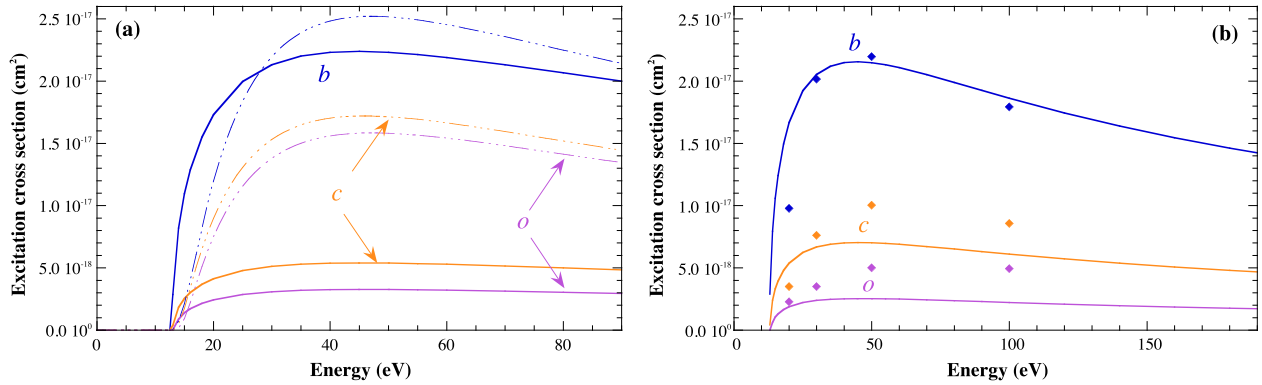

Fig. (1). Total cross section (*solid lines*) for excitation to the $^1\Pi_u$ states from the $\upsilon''=0$ level of the ground state of N_2 molecule as a function of collision energy, compared with (**a**) theoretical [19] (*dashed-dotted lines*) and (**b**) experimental [16] (*close diamonds*) results in literature. In (**b**) total cross sections have been obtained using a de-coupled scheme for assigment (see text for details).

An interesting point is the investigation of the role of vibronic coupling in changing the dependence of the excitation on vibrational quantum states. In Fig. (**2**) the state-to-state cross section for a transition from the $\upsilon''=0$ level to the vibrational levels of the *b* state, at the collision energy of 200 eV, is shown. The pattern of the final vibrational profile is strongly irregular, due to the coupling perturbation, and far from the expected bell-shape behavior, usually observed for transitions from the fundamental vibrational level. In this case the experimental state-to-state cross sections by Zipf [24] confirm the vibrational pattern. In particular the coincidence of cross section peaks for specific υ' levels is observed, though the theoretical calculations predicts lower absolute values. It should be stressed that first order approaches are expected to be predictive at high collision energies, however results prove the possibility of using the similarity approach in systems characterized by a perturbed vibrational progression due to vibronic coupling.

Fig. (**2b**) reports the state-to-state cross sections for the excitation transitions populating the $\upsilon''=1$ level and originating the emission in the Birge-Hopfield system [24]. The cross sections follow the complex behavior of the vibronic transition moment elements and, due to the relative position of the potential energy curves for the ground and excited states and to the monotonic decrease of the diabatic transition dipole moment with the *R*-coordinate [15], the vibrational excitation for this system does not result in cross section enhancement.

For the $^1\Sigma_u^+$ complex, the cross sections for the b' and c' components are comparable, while those for the e' state are considerably lower (Fig. **3a**). In Fig. (**3b**) the excitation to the b' state from $\upsilon''=0$ level is compared with experimental integral cross sections in ref. [17] obtained by electron-energy loss spectroscopy allowing for the detection of a limited number of vibrational levels (υ'' [0-10]), and with the estimated full-integral cross section, equivalent to υ'' [0-16]. The large discrepancy is attributed to the inclusion in the theoretical cross section of excitations to higher vibrational levels lying outside the spectral energy range explored by experiments. In fact, the theoretical cross sections of Fig. (**3**), obtained by including in the summation

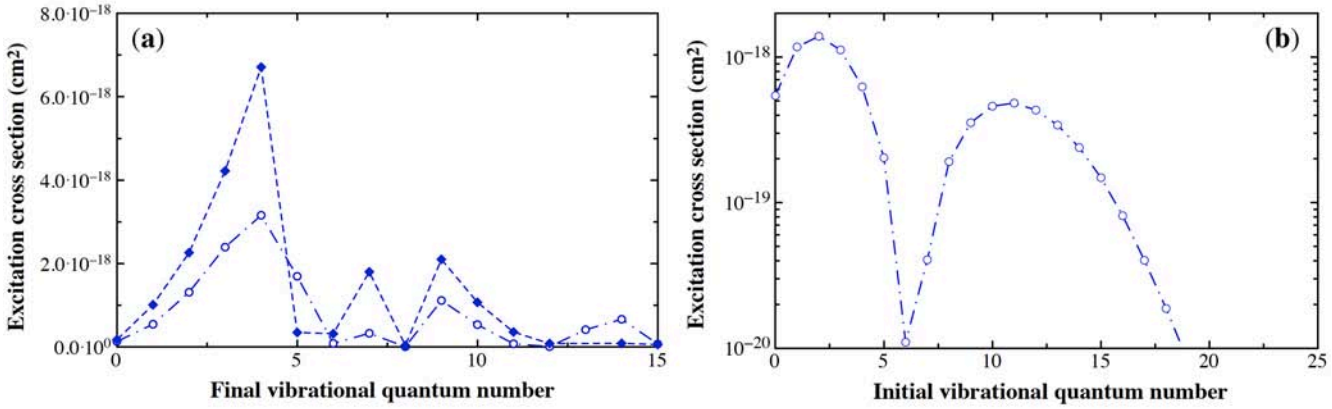

Fig. (2). (**a**) Excitation cross section (*open circles*) from the $\upsilon''=0$ level of the ground state to the $b\,^1\Pi_u$ state of N_2 molecule, as a function of final vibrational quantum number υ', at collision energy $E=200$ eV, compared with experimental results (*closed diamonds*) of ref. [24]. (**b**) Excitation cross section to the $\upsilon'=1$ level of the $b\,^1\Pi_u$ state of N_2 molecule, as a function of initial vibrational quantum number, at collision energy E=200 eV.

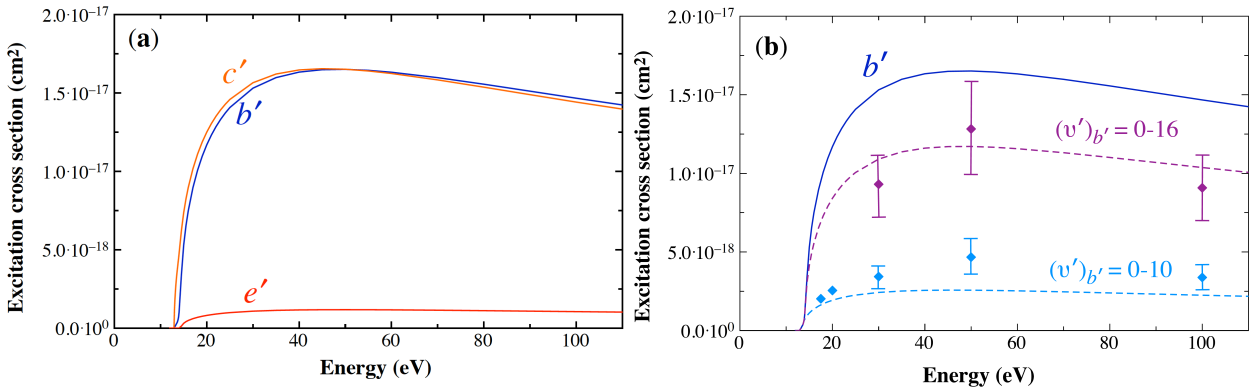

Fig. (3). (**a**) Total cross section for excitation to the $^1\Sigma_u^+$ states from the υ''=0 level of the ground state of N_2 molecule as a function of collision energy. (b) Cross section for excitation to the $b'^1\Sigma_u^+$ state from the υ''=0 level (*solid line*), compared with experimental results in ref. [17] (close diamonds). Cross sections obtained considering a variable number of final vibrational levels are also shown (dashed lines).

of Eq. (8) a reduced number of final vibrational levels (dashed lines), are found to be in better agreement with the experiments.

PART II: RESONANT COLLISIONS

5. ELECTRON-IMPACT VIBRATIONAL EXCITATIONS FOR CO_2 MOLECULE: THEORETICAL MODEL

The low energy integrated cross section, for electron-CO_2 scattering, shows two distinctive features: a $^2\Pi_u$ shape resonance around 3.8 eV (see for example refs. [25-28]) and, at energies below 2 eV, an enhancement due to the presence of the $^2\Sigma_g^+$ symmetry virtual state [29-32]. Both phenomena give rise to a temporary CO_2 system. For a general review see ref. [33] and references therein. In this section we report the electron-CO_2 resonant vibrational-excitation process, *via* $^2\Pi_u$ shape resonance,

$$e^- + CO_2(X\,^1\Sigma_g^+, v_i) \rightarrow CO_2^-(^2\Pi_u) \rightarrow e^- + CO_2(X\,^1\Sigma_g^+, v_f), \quad (10)$$

where $\upsilon_i(\upsilon_f)$ represents the initial (final) vibrational level of the ground state of CO_2. In its ground electronic state the CO_2 molecule has a linear geometry (D_{2h}) and it has three vibrational normal modes: symmetric stretching, bending mode and asymmetric stretching. The doubly degenerate $^2\Pi_u$ symmetry of CO_2^- splits the bending mode into two (Renner-Teller) non-degenerate $^2A_1$ and $^2B_1$ components ($C_{2\upsilon}$ symmetry) [34]. In principle, as the CO_2 is a polyatomic molecule, the scattering cannot be described by a simple one-dimensional model, but it needs a multidimensional treatment of the nuclear motion. However, the present preliminary calculations are limited to a one-dimensional model where the symmetric stretch is decoupled from the two bending modes (see sec. 6). This permits the use of the local complex-potential model for cross section calculations, in its standard formulation for diatomic molecules [7]. Below the relevant equations are briefly illustrated.

The Schrödinger-like equation for the resonant nuclear wave function $\xi(R)$, is given by

$$\left(T_N + V^- + \Delta - \frac{i}{2}\Gamma - E\right)\xi(R) = -V_k(R)\,\chi_i(R), \quad (11)$$

where E is the total energy and T_N denotes the nuclear kinetic energy operator. $V^- + \Delta - \frac{i}{2}\Gamma$ is the *optical complex potential* where the real part, V^-, is the adiabatic electronic potential for the resonant state, Δ is the level shift and the imaginary part, Γ, is the width of the resonance. All these quantities parametrically depend on the internuclear distance R. In the present calculations the level shift $\Delta(R)$ is assumed included in the resonant potential $V^-(R)$ [7]. Moreover, $\chi_i(R)$ is the initial vibrational wave function of the neutral molecule, and $V_k(R)$ is the discrete-continuum coupling matrix element depending on the incident electron momentum k.

The scattering T -matrix can then be written as:

$$T_{if}(E) = \langle \chi_f^* | V_k(R) | \xi \rangle \quad (12)$$

and the total cross section can be finally calculated by [27]

$$\sigma_{\upsilon_i,\upsilon_f} = \frac{4\pi^3}{k^2} | T_{if} |^2 . \quad (13)$$

6. ELECTRON-CO_2 RESULTS

A common feature of polyatomic molecules, which is consequence of the multidimensional nature of the system, is the so-called stretch-bend 'Fermi resonance', which refers to an accidental degeneracy between certain vibrational modes. In the case of CO_2, the first Fermi resonance is between the pure symmetric stretching mode (1,0,0) and pure bending mode (0,2,0) which are nearly degenerate (Fermi dyad) and they mix, about 50%, to form two physical states [28, 34]. In the following we ignore this mixing and only address the symmetric stretching mode.

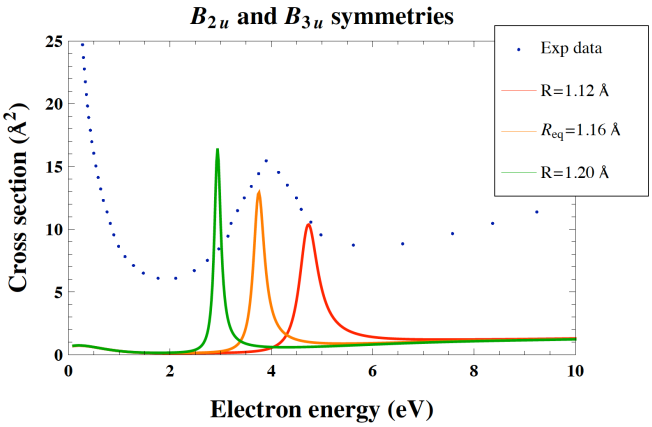

Fig. (4). Electron-CO_2 total cross section for the degenerate B_{2u} and B_{3u} symmetries of D_{2h}, calculated at three different internuclear distances. The experimental data are taken from ref. [33].

The CO_2 potential energy curve was calculated using MOLPRO [35], an aug-cc-pVQZ basis and the coupled-cluster model. The UK polyatomic R-matrix code of UK-R-matrix code [36, 37] was used for the scattering calculations. A Static Exchange plus Polarization (SEP) model, and the same basis used for CO_2, was used to calculate the complex potential energy curve for CO_2^-. The R-matrix calculations were performed on a grid of fixed internuclear distances. The position and width of the resonant state was then calculated by fitting the corresponding eigenphases sum with a Breit-Wigner function [38]. The resonance curve for the symmetric stretch was obtained by changing the internuclear C-O separation. Fig. (**4**) shows the total cross sections, corresponding to the eigenphases calculated at three different geometries and for two degenerate symmetries, B_{2u} and B_{3u}, of D_{2h} group. The position of the theoretical peak at equilibrium distance is close to the maximum in the experimental data and the peak position shifts as the internuclear distance changes.

The computed potential energy curves for CO_2 and CO_2^- are reported in Fig. (**5**) with the resonance width $\Gamma(R)$.

The 'boomerang effect' indicates that the resonance lifetime is about equal to the period of the linear symmetrical-stretching oscillation; using this observation it is justified, in a first approximation, to reduce the multidimensional problem of vibrational excitation in CO_2 to a simpler problem in one dimension involving only the linear symmetric-stretch coordinate [26]. Figs. (**6**, **7**) show some preliminary results for symmetric stretching cross sections calculated for the excitation to the first few vibrational levels. In particular Fig. (**6**) compares the present calculated cross sections for the elastic transition $(0,0,0)\rightarrow(0,0,0)$ with both the 1-dimensional boomerang model and a multi-dimensional calculations of ref. [34]. Fig. (**7**) shows the calculated inelastic cross sections for the pure $(0,0,0)\rightarrow(1,0,0)$ and $(0,0,0)\rightarrow(2,0,0)$ transitions.

Fig. (**8**) shows the cross sections (left panel) and the corresponding rate coefficients (right panel) as a function of the electron energy, for the vibrational transitions $(0,0,0)\rightarrow(\upsilon_f,0,0)$, where $\upsilon_f = 0,1,2,5,10$. The rate coefficients were calculated by assuming a Maxwellian electron energy distribution function. The typical decreasing trend with the final vibrational levels is observed in both the figures.

Calculations have been performed also for the RVE processes starting from excited vibrational levels. Figs. (**9**, **10**) show the cross sections and the corresponding rate coefficients for the transitions $(\upsilon_i,0,0)\rightarrow(\upsilon_f,0,0)$, with $\upsilon_i = 1$ and 2 respectively and $\upsilon_i \le \upsilon_f \le 5$. The cross sections, when compared with those of Fig. (**8**), exhibit new structure which overlaps the rapid oscillations. Two and three broad maxima are observed in the cross section curves of Figs. (**9**, **10**) respectively, probably generated by the behavior of the corresponding wave functions of the initial vibrational levels. The rate coefficients, on the other hand, are not so strongly dependent on the initial vibrational quantum number: the trend with electron temperature and the absolute values are similar for all transitions.

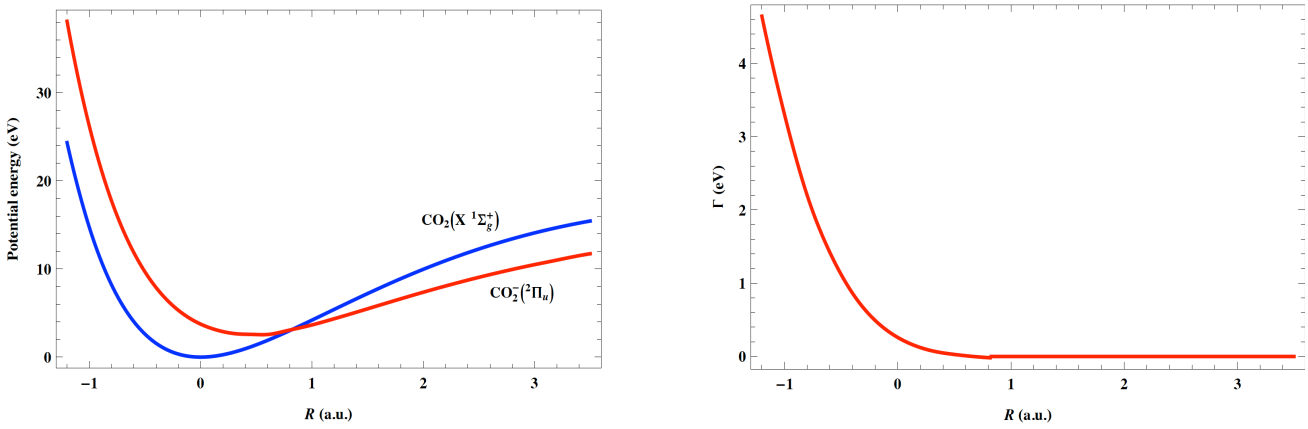

Fig. (5). Curves for the symmetric stretching mode: Left, potential energy curves for CO_2 and CO_2^-; Right, the corresponding resonance width. Both quantities are shown as a function of the displacement from the equilibrium O-O distance, which is twice the C-O bond length.

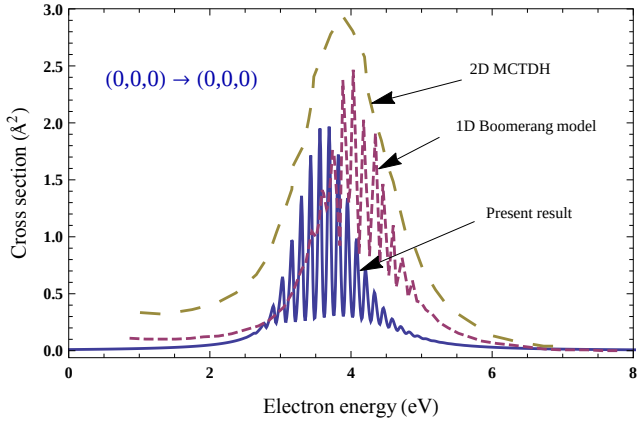

Fig. (6). Elastic electron-CO_2 resonant cross section: solid line refers to the present 1-dimensional results, short-dashed line is a 1D boomerang model and the long-dashed line is a multidimensional calculation (MCTDH) [34].

7. ELECTRON-DIATOMIC MOLECULES RESONANT COLLISIONS

A brief review on electron-molecule collisions is presented in this section. The aim is to provide a general survey on the most recent advances in cross section and rate coefficient calculations relevant for atmospheric plasmas.

7.1. N_2, NO and O_2 molecules

Electron-impact cross sections and rate coefficients have also been calculated for diatomic nitrogen, nitric oxide and oxygen molecules, relevant for terrestrial atmosphere. The calculations were performed for the following RVE processes, linking different ground state vibrational levels [5, 10],

$$e^- + \mathrm{N}_2(\mathrm{X}\,^1\Sigma_g^+, \upsilon_i = 0-64, J) \rightarrow \mathrm{N}_2^-(\mathrm{X}\,^2\Pi_g) \rightarrow e^- + \mathrm{N}_2(\mathrm{X}\,^1\Sigma_g^+, \upsilon_f = 0-64, J), \quad (14)$$

$$e^- + \mathrm{NO}(\mathrm{X}\,^2\Pi, \upsilon_i = 0-54, J) \rightarrow \mathrm{NO}^-(^3\Sigma^-, ^1\Delta, ^1\Sigma^+) \rightarrow e^- + \mathrm{NO}(\mathrm{X}\,^2\Pi, \upsilon_f = 0-54, J), \quad (15)$$

$$e^- + \mathrm{O}_2(\mathrm{X}\,^3\Sigma_g^-, \upsilon_i = 0-41, J) \rightarrow \mathrm{O}_2^-(^2\Pi_g, ^2\Pi_u, ^4\Sigma_u^-, ^2\Sigma_u^-) \rightarrow e^- + \mathrm{O}_2(\mathrm{X}\,^3\Sigma_g^-, v_f = 0-41, J), \quad (16)$$

where, in all cases, the molecule, initially in the (v_i, J) ro-vibrational level, is excited by electron-impact to the final

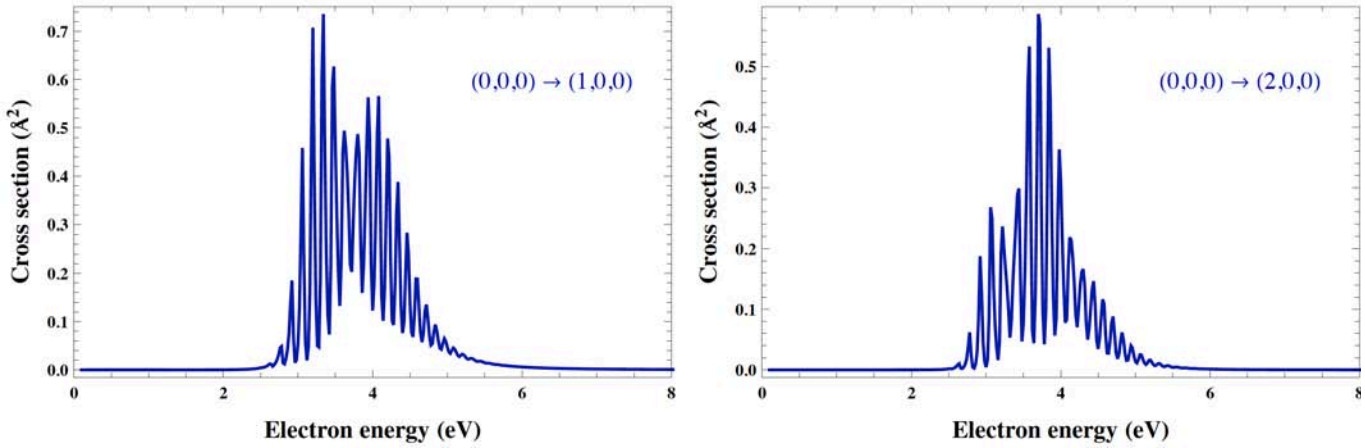

Fig. (7). Cross sections for the pure linear symmetric stretching $(0,0,0) \rightarrow (1,0,0)$ and $(0,0,0) \rightarrow (2,0,0)$ transition.

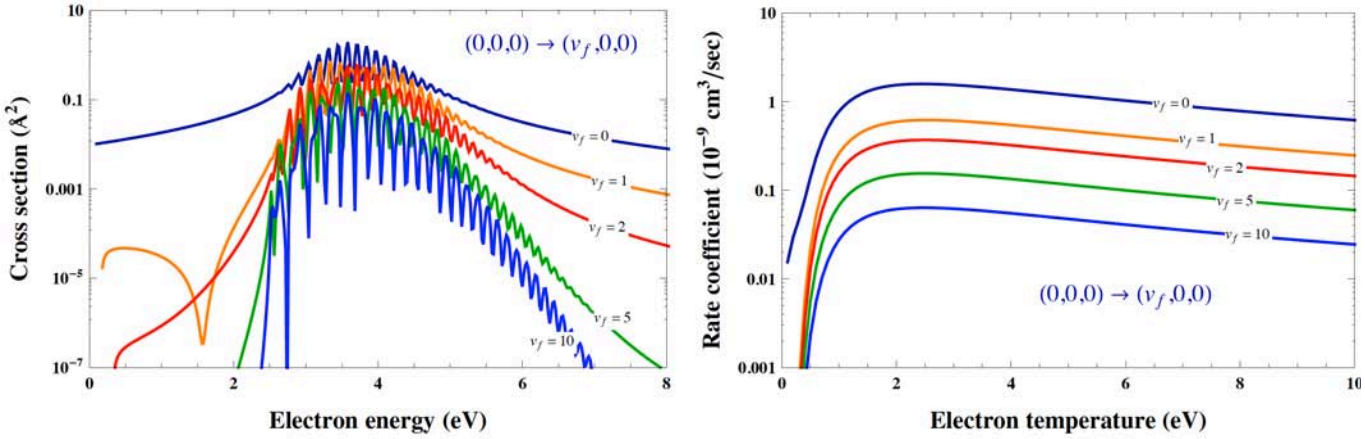

Fig. (8). Electron-CO_2 cross sections (left panel) and rate coefficients (right panel) are shown for the transition $(0,0,0) \rightarrow (\upsilon_f,0,0)$ where $\upsilon_f = 0,1,2,5,10$.

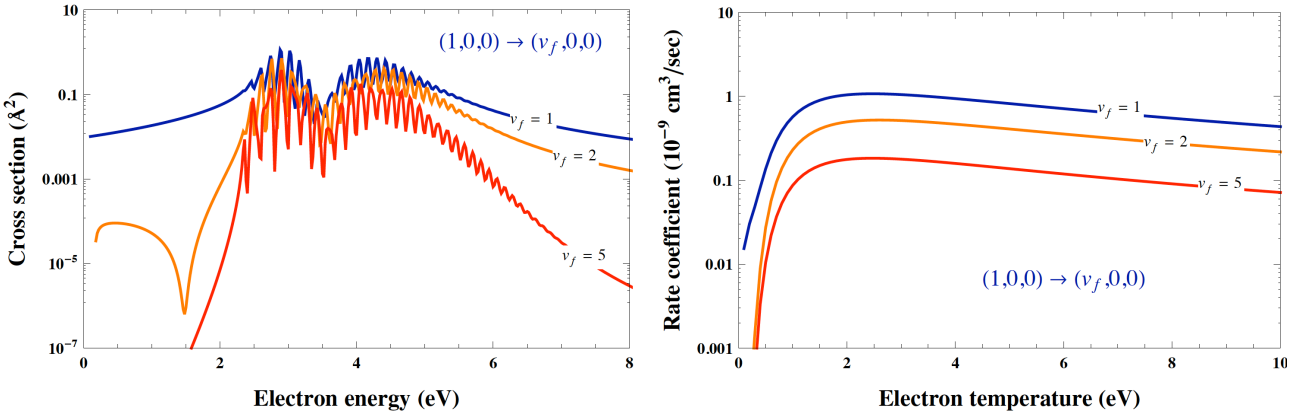

Fig. (9). Same as Fig. (**8**) for the transition $(1,0,0) \rightarrow (\upsilon_f,0,0)$ where $\upsilon_f = 1,2,5$.

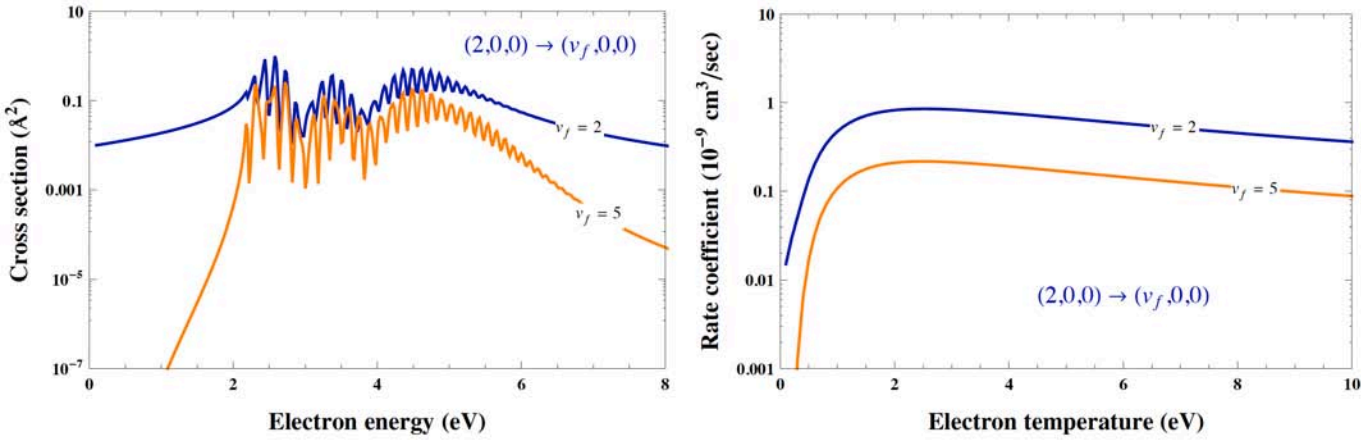

Fig. (10). Same as Fig. (**8**) for the transition $(2,0,0) \rightarrow (\upsilon_f,0,0)$ where $\upsilon_f = 2,5$.

level (υ_f, J). The range of the vibrational quantum numbers is shown in parenthesis. The process for N_2 occurs through the formation of the resonant state $N_2^-(^2\Pi_g)$, while in the case of NO and O_2 multiple contributions come from the three states $^3\Sigma^-, ^1\Delta, ^1\Sigma^+$ for NO and from the four resonant states $^2\Pi_g, ^2\Pi_u, ^4\Sigma_u^-, ^2\Sigma_u^-$ for O_2. A complete account of the calculations is reported in refs. [5, 10]. Here we limit ourselves only to the discussion of some relevant result.

The RVE calculations were extended to all the possible transitions $(\upsilon_i, J) \rightarrow (\upsilon_f, J)$ among all the vibrational levels, and for fixed different J values (rotationally elastic processes) running from 0 to 150 for N_2 and NO and from 1 to 151 for O_2 as allowed by nuclear symmetry considerations [10]. Examples of cross sections for process (14) are shown in Fig. (**11a**, **b**), for some elastic and inelastic transitions respectively. An evident feature is the strong oscillations present in all the curves which reproduce the vibrational structures of the resonant state $N_2^-(X\,^2\Pi_g)$. The cross section peaks, in fact, are placed at an energy corresponding to the resonant vibrational eigenvalues of N_2^- [9]. These structures disappear abruptly at the energy threshold of the vibrational continuum of the resonant state. Correspondingly, Fig. (**11c**, **d**) shows the rate coefficients for the transitions given in Fig. (**11a**, **b**), calculated by adopting a Maxwellian electron energy distribution function. The rates show a very smooth behavior and no memory is retained of the vibrational oscillations in the cross sections.

The trend with respect to the vibrational quantum number is that expected for resonant collisions. In fact, the rates and the cross sections decrease as the vibrational level is increased.

This, in a simplified model for resonant collisions [39], is probably due to the product of the Franck-Condon factors for the two transitions $\upsilon_i \rightarrow \upsilon_r$ and $\upsilon_r \rightarrow \upsilon_f$, ($\upsilon_r$ is the resonance vibrational level) involved in the process. The Franck-Condon overlap, in fact, is expected to reduce as the υ_i or υ_f vibrational levels increase, due to the increasingly rapid wave function oscillations.

Analogous comments hold for the cross sections and rates for RVE process (15) involving NO molecules, shown in Fig. (**12a**, **b**).

The RVE process (16) for the O_2 molecule gives the cross sections shown in Fig. (**13**). These display fast oscillations below ~4 eV which are strongly reduced, but still present, for energies above this value. These structures are due to the different contributions, in different energy

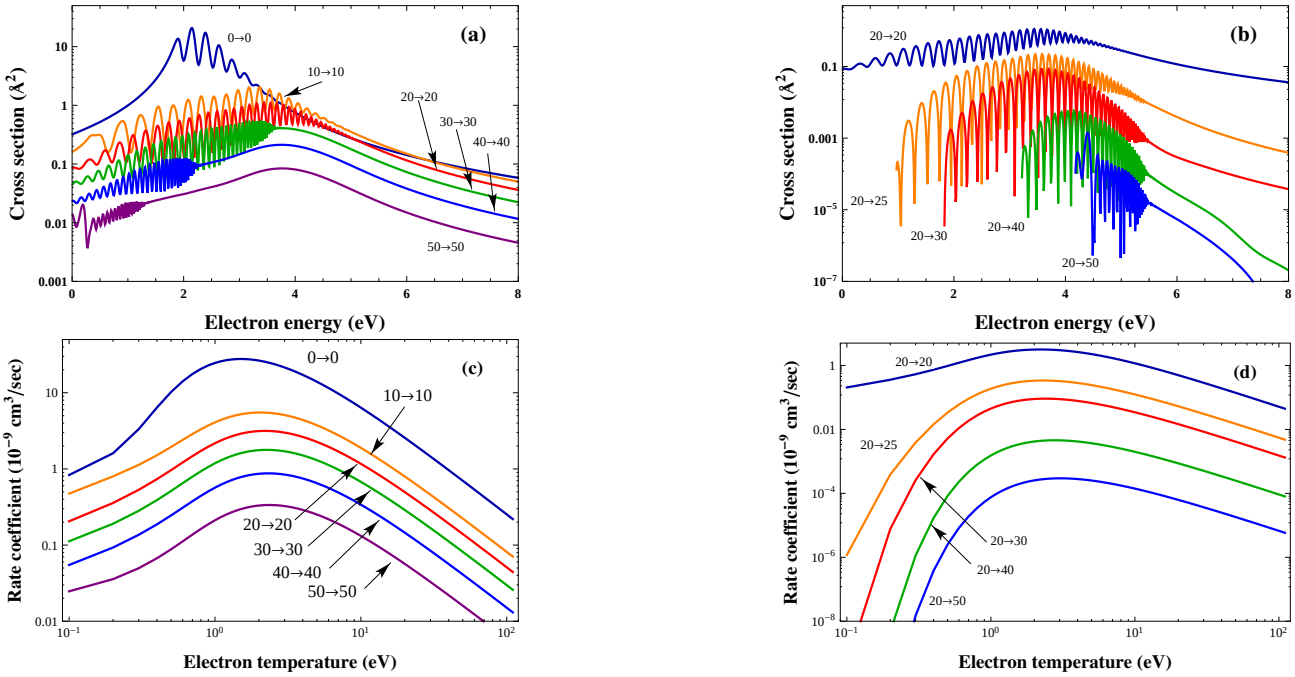

Fig. (11). Resonant e-N_2 vibrational excitation cross sections (**a**, **b**) and corresponding rate coefficients (**c**, **d**) for $\upsilon_i = \upsilon_f$ and $\upsilon_i = 20 \rightarrow \upsilon_f \geq \upsilon_i$, respectively. The rotational quantum number is set to $J = 0$.

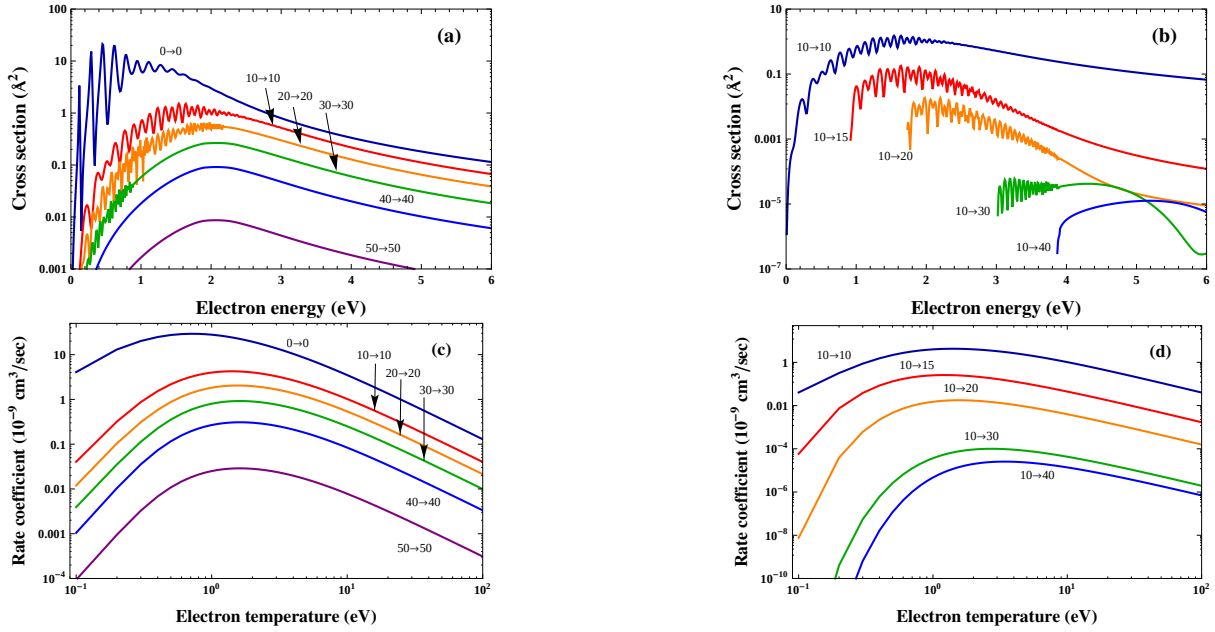

Fig. (12). Same as Fig. (**11**) for NO molecule.

ranges, coming from the four resonant states involved in the process. For this molecule the rates for the excitation of low υ_i states also show some structure.

7.2. CO Molecule

Cross sections and rate coefficients were calculated also for the resonant vibrational excitations involving the vibrationally excited CO molecule. This species, together with carbon dioxide, is the main component of the Venusian and Martian atmospheres. The process considered is,

$$e^- + \mathrm{CO}(\mathrm{X}\,^1\Sigma^+, \upsilon_i = 0-80) \rightarrow \mathrm{CO}^-(^2\Pi) \rightarrow e^- + \mathrm{CO}(\mathrm{X}\,^1\Sigma^+, \upsilon_f = 0-80), \quad (17)$$

occurring through the resonant state $\mathrm{CO}^-(^2\Pi)$ and involving 81 vibrational levels. Cross sections and rates, shown in

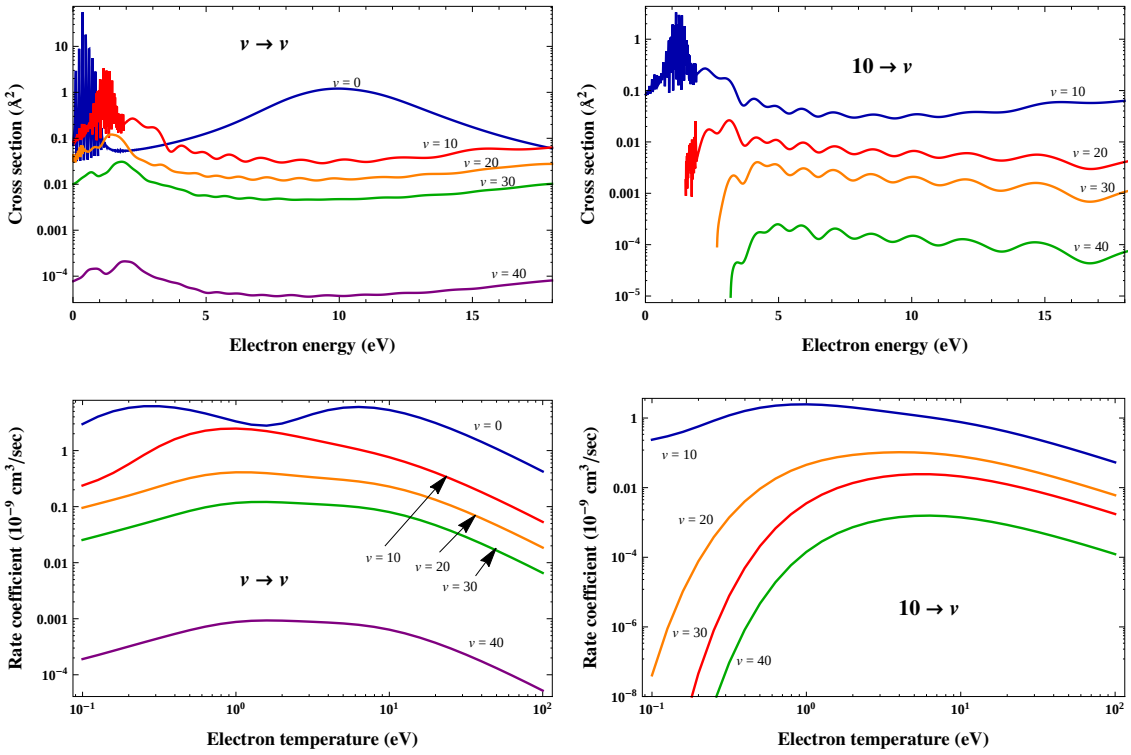

Fig. (13). Same as Fig. (**11**) for O_2 molecule with $J=1$ allowed by nuclear symmetry [10].

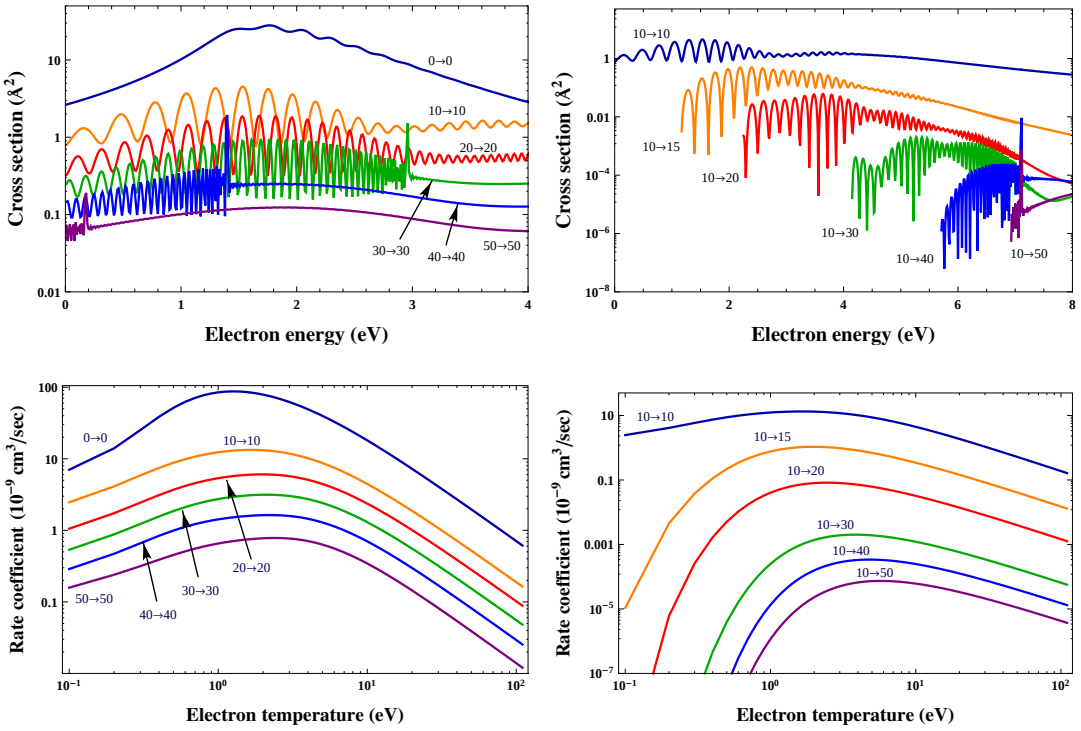

Fig. (14). Same as Fig. (**11**) for CO molecule with $J=0$.

Fig. (**14**), are quite similar to the previous cases, except for the appearance of sharp peaks just below the vibrational continuum of the resonant state for some transitions.

7.3. Single Quantum Transitions

The RVE elastic transitions show the largest cross sections and rates. However they play no role in

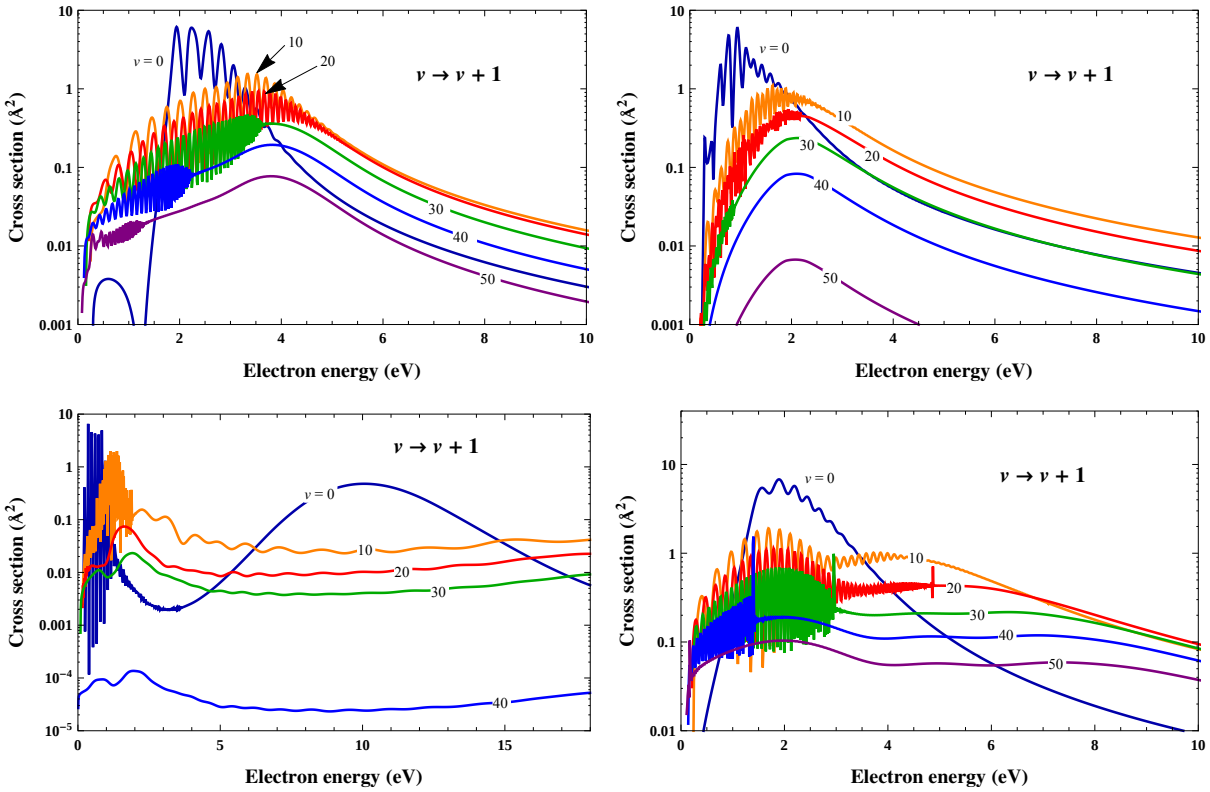

Fig. (15). RVE cross sections for the single quantum excitations ($\Delta v = 1$) in N_2 (upper-left panel), NO (upper-right panel), O_2 (lower-left panel), CO (lower-right panel).

redistributing energy among the internal degrees of freedom of the molecular species. The major role, in this case, is played by transitions which change the vibrational state by just one quantum, $\upsilon_i \rightarrow \upsilon_i \pm 1$, whose cross sections are comparable with the elastic ones. Figs. (**15**, **16**) show the cross sections and the corresponding rates coefficients for the transitions $\upsilon_i \rightarrow \upsilon_i + 1$ for the RVE processes involving the diatomic molecules.

7.4. H_2 Molecule

Resonant processes for H_2 molecule, the main component of the giant planets, have been studied over a long period. This has resulted in a vast theoretical and experimental literature on the topic, stimulated by the importance of hydrogen plasmas for both astrophysical and technological research. Sets of cross sections and rate coefficients have been calculated for $H_2(\upsilon_i)$ by different authors [40-44] for dissociative attachment and vibrational excitations according to the reactions,

$$e^- + H_2(X\,^1\Sigma_g^+, \upsilon_i = 0-14) \rightarrow H_2^-(X\,^2\Sigma_u^+) \rightarrow H(1s) + H^-(1s^2), \quad (18)$$

$$e^- + H_2(X\,^1\Sigma_g^+, \upsilon_i = 0-14) \rightarrow H_2^-(X\,^2\Sigma_u^+) \rightarrow e^- + H_2(X\,^1\Sigma_g^+, \upsilon_f = 0-14), \quad (19)$$

both occurring through the ground resonant electronic state $X\,^2\Sigma_u^+$ of the H_2^- ion. Calculations have also been extended to the process involving the first excited valence state $B\,^2\Sigma_g^+$ [45] and to RVE leading to electron impact dissociation of H_2 [42, 46-48].

More recently, cross sections for DEA and RVE processes, involving a Rydberg excited resonance, were calculated in refs. [7-9]. Complete sets of *ab initio* cross sections and rate coefficients were obtained for the process

$$e^- + H_2(X\,^1\Sigma_g^+, \upsilon_i = 0-14) \rightarrow H_2^-(^2\Sigma_g^+) \rightarrow H(n=2) + H^-(1s^2), \quad (20)$$

occurring through the Rydberg excited $H_2^-(^2\Sigma_g^+)$, and yielding to the production of a negative ion and an excited atom. Cross sections and rates are shown in Fig. (**17**). In this case the cross sections for $v_i = 0$ shows the smallest values. For high levels ($\upsilon_i > 5$) oscillations start to appear in the cross sections mainly determined by the vibrational continuum of the Rydberg state [9]. The variation of the rates with the vibrational quantum number is contained, at the peaks, within a factor of 100. This behavior is quite different for the case of the shape resonance in process (18) where, as is well-known, the rates increase with the initial vibrational levels by several orders of magnitude [45].

Differential cross sections were calculated also for RVE process occurring *via* the Rydberg resonance [7], namely,

$$e^- + H_2(X\,^1\Sigma_g^+, \upsilon_i = 0) \rightarrow H_2^-(^2\Sigma_g^+) \rightarrow$$
$$e^- + H_2(X\,^1\Sigma_g^+, \upsilon_i = 0 - 14). \quad (21)$$

The cross sections have been obtained only for the transition $0 \rightarrow \upsilon_f = 0 - 14$. In Fig. (**18**) the differential RVE cross sections are shown for υ_f = 4, 5, 6, 7, at a scattering angle of 85°. The theoretical calculations are in satisfactory agreement with the experimental data [39]. Extension to all the vibrational transitions ($\upsilon_i, \upsilon_f > 0$) has been recently published in Ref. [49].

CONCLUSION

Non-resonant electron-impact total cross sections are presented for the vibro-electronic excitation of the N_2 ($X\,^1\Sigma_g^+$) molecule to the electronic states $b,c,o\,^1\Pi_u$ and $b',c',e'^1\Sigma_u^+$, taking into account the coupling among the three states for each symmetry. The results obtained are compared with previous (uncoupled) calculations and with experiment. For the $^1\Pi_u$ symmetry, good agreement for cross sections is found for the b state with the results obtained by the Gryzinski method. Some discrepancy is observed however for the c and o states. This is attributed to the lower number of vibrational levels included in the present calculations, which recognize that higher levels lead to dissociation through a predissociation mechanism involving the continuum of the b states. Any comparison with experiments must take into account both the limited number of vibrational levels observed in the measurements and the emission intensity assignment which, as reported in literature, has been applied within a state-decoupled frame. Once these two restrictions are implemented in the preset theoretical calculations, the resulting cross sections are to be found in good agreement with the experimental data.

Good agreement with the experiments is found also for the excitation to the $^1\Sigma_u^+$ state of N_2. However, the comparison with the measurements again required the inclusion of a lower number of vibrational levels in the calculations, in order to make the theoretical results consistent with the experiments.

Electron-impact theoretical cross sections and rate coefficients, for the resonant vibration excitation, for the symmetric stretching mode of the CO_2 molecule only, are calculated using the *local complex-potential* model for resonant collisions. The potential curves for both CO_2 ($X\,^1\Sigma_g^+$) molecule and $CO_2^-(^2\Pi_u)$ resonant state are calculated using the MOLPRO electronic structure code. Resonance positions and widths are calculated by using the

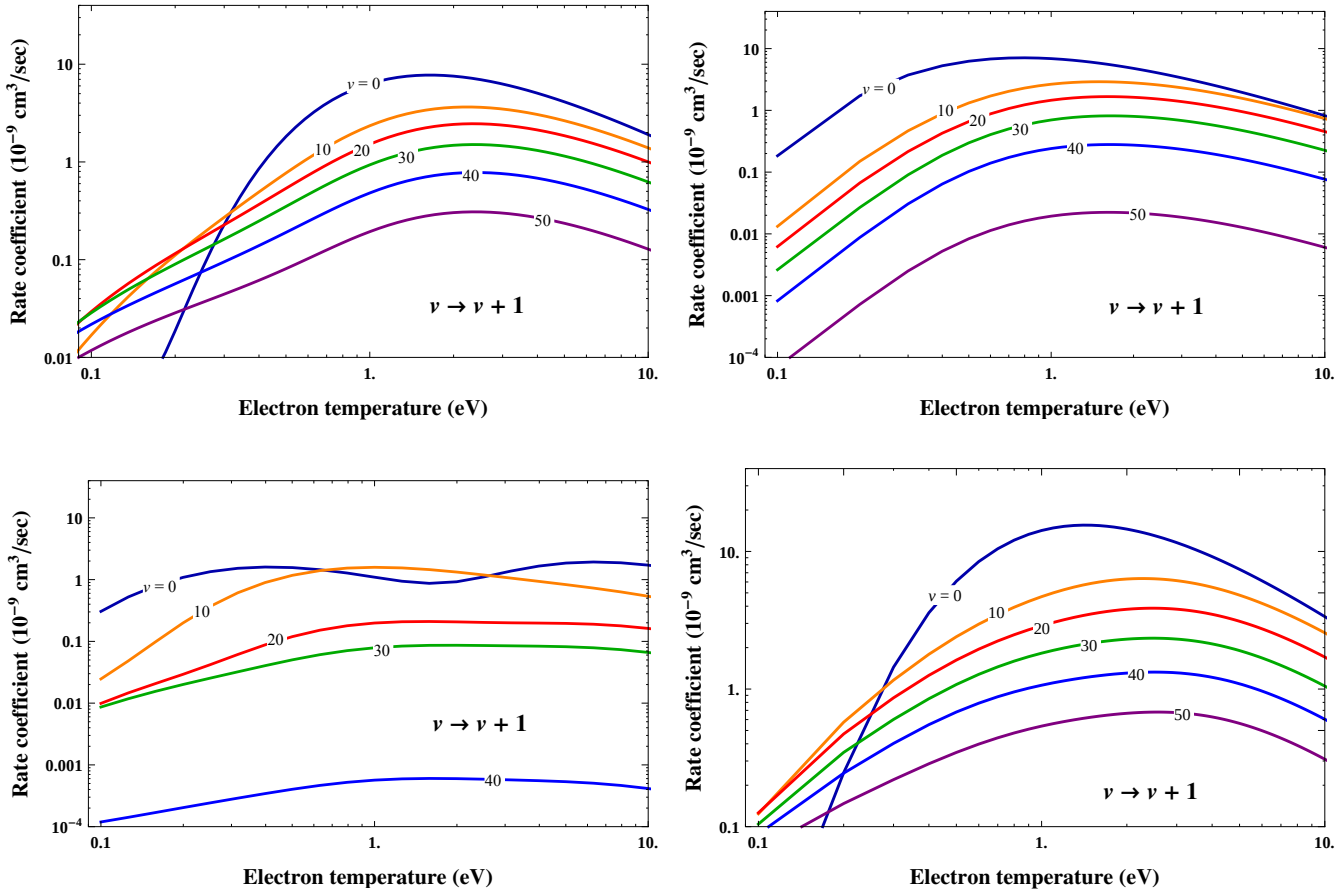

Fig. (16). Same as Fig. (**15**) for the rate coefficients.

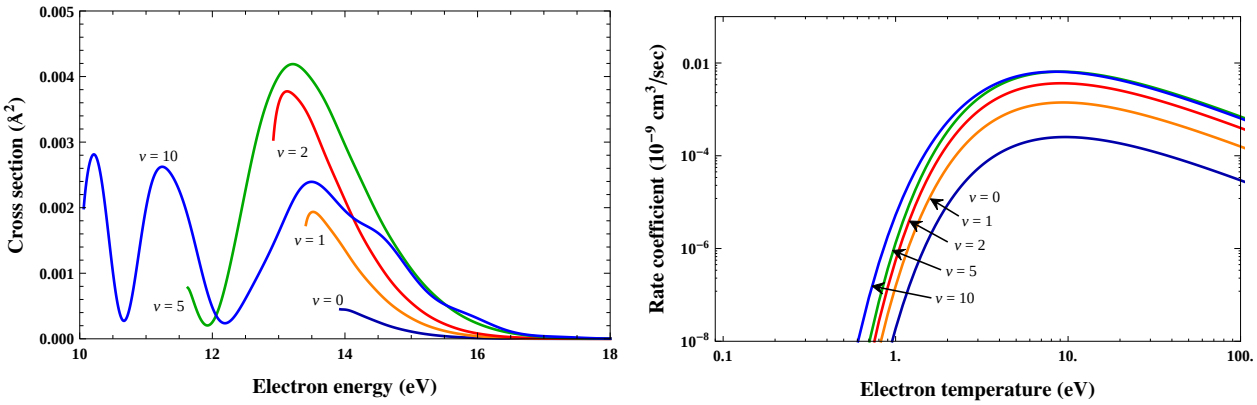

Fig. (17). Resonant e-H_2 dissociative attachment cross sections (left panel) and corresponding rate coefficients (right panel) for process (20). For clarity, the cross sections and rates are shown for some of the vibrational levels, as indicated in the figure.

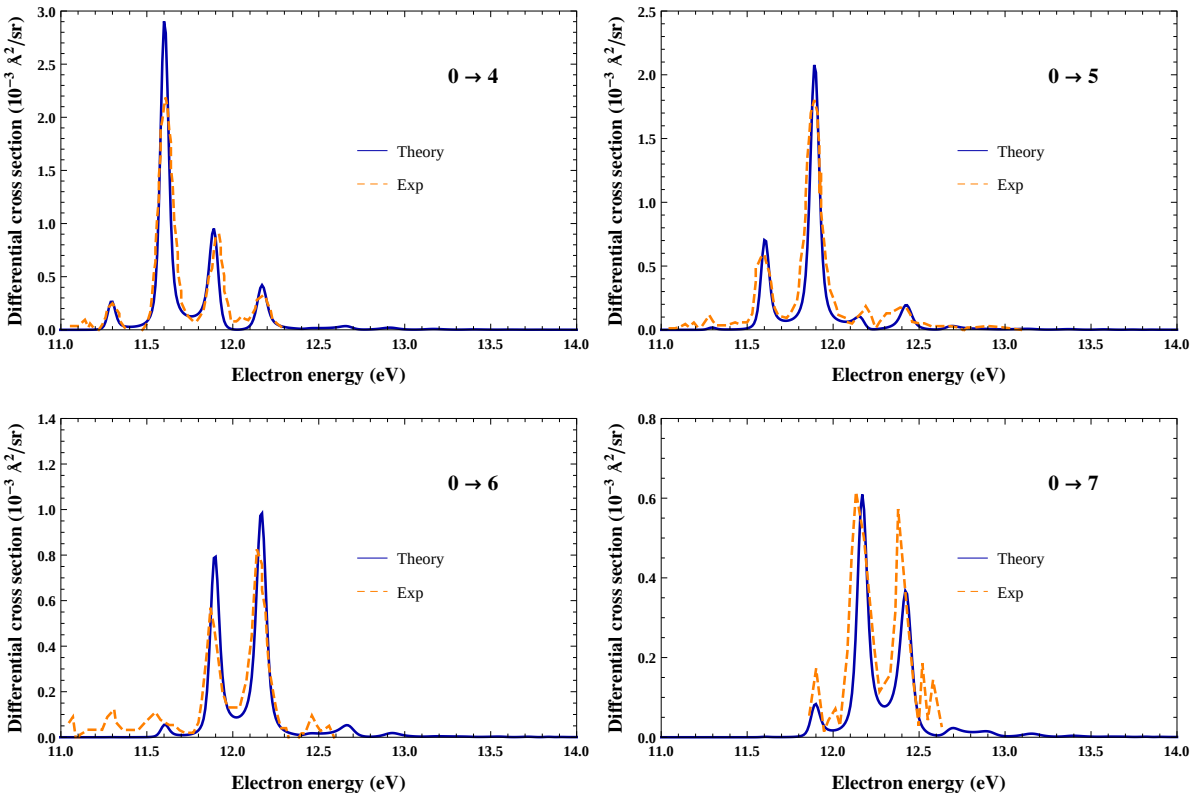

Fig. (18). Differential cross sections at a scattering angle of 85 ^{o} for the resonant vibrational excitation of H_2 molecule through the process (21) for the transition $0 \rightarrow \upsilon_f = 4,5,6,7$. The theoretical calculations (solid lines) [7] are compared with the experimental data (*dashed lines*) [39].

R-matrix method. The cross sections obtained are found to be in good agreement with previous theoretical calculations and with experiment. Rate coefficients are also calculated for the transition $(0,0,0) \rightarrow (\upsilon_f,0,0)$ with $\upsilon_f = 0,1,2,5,10$, for electron temperatures below 10 eV. No experimental or theoretical data are available for comparison with these rates.

The calculations presented in this work aim to provide input data (cross sections and rate coefficients) for models of planetary atmospheres and, in particular, are intended to acquire knowledge and information useful for (re)-entry problems in space exploration. It is with this perspective that we review all the recent calculations performed by our collaboration for different molecules. In particular we have considered the resonant vibrational excitation of N_2, O_2 and

NO by electron impact, important for the Earth re-entry conditions, and of CO molecule, which, together with carbon dioxide, is the main component of the atmospheres of Mars and Venus. Finally, we also review the resonant vibrational excitations and dissociative electron attachment processes for H_2 molecule, the main component of gaseous planets, occurring through the $^2\Sigma_g^+$ Rydberg-excited electronic state of H_2^- molecular ion. The RVE cross section calculations, for this system, are presently limited to transitions starting from the $\upsilon_i = 0$ only. Extension of calculations to the other levels ($\upsilon_i > 0$) are reported in [49].

The full set of numerical cross sections and rate coefficients, presented in this paper, is available at the website: http://users.ba.cnr.it/imip/cscpal38/phys4entry/database.html

CONFLICT OF INTEREST

The authors confirm that this article content has no conflicts of interest.

ACKNOWLEDGEMENTS

The present research has received funding from the European Community's Seventh Framework Programme (FP7/2007-2013) under grant agreement number 242311. One of the authors (AL) would also like to thank support from contract C505-IMIP under ESA Contract 21029.

REFERENCES

[1] Capitelli M, Celiberto R, Esposito F, Laricchiuta A. Molecular dynamics for state-to-state kinetics of non-equilibrium molecular plasmas: state of art and perspectives. Plasma Process Polym 2009; 6(5): 279-94.

[2] Shimamura I, Takayanagi K. Electron-molecule collisions. New York and London: Plenum Press 1984.

[3] Celiberto R. Electron-molecule collision processes in non-equilibrium molecular plasmas. In: ESCAMPIG XXI, Viana do Castelo, Portugal 2012: pp. 10-4

[4] Capitelli M, Celiberto R, Colonna G, *et al*. Plasma kinetics in molecular plasmas and modeling of reentry plasmas. Plasma Phys Control Fusion 2011; 53(12):124007.

[5] Laporta V, Celiberto R, Wadehra JM. Theoretical vibrational-excitation cross sections and rate coefficients for electron-impact resonant collisions involving rovibrationally excited N_2 and NO molecules. Plasma Sources Sci Technol 2012; 21(5): 055018.

[6] Laporta V, Cassidy CM, Tennyson J, Celiberto R. Electron-impact resonant vibration excitation cross sections and rate coefficients for carbon monoxide. Plasma Sources Sci Technol 2012; 21(4): 045005.

[7] Celiberto R, Janev RK, Wadehra JM, Laricchiuta A. Cross sections for 11-14-eV e-H_2 resonant collisions: Vibrational excitation. Phys Rev A 2008; 77(1): 012714.

[8] Celiberto R, Janev RK, Wadehra JM, Laricchiuta A. Cross sections for 14-eV e-H_2 resonant collisions: Dissociative electron attachment. Phys Rev A 2009; 80: 012712.

[9] Celiberto R, Janev RK, Wadehra JM, Tennyson J. Dissociative electron attachment to vibrationally excited H_2 molecules involving the $^2\Sigma_g^+$ resonant Rydberg electronic state. Chem Phys 2012; 398: 206-13.

[10] Laporta V, Celiberto R, Tennyson J. Resonant vibrational-excitation cross sections and rate constants for low-energy electron scattering by molecular oxygen. Plasma Sources Sci Tech 2013; 22(2): 025001.

[11] Ermler WC, McLean AD, Mulliken RS. Ab initio study of valence-state potential energy curves of nitrogen. J Phys Chem 1982; 86(8): 1305-14.

[12] Stahel D, Leoni M, Dressler K. Nonadiabatic representations of the $^1\Sigma_u^+$ and $^1\Pi_u$ states of the N_2 molecule. J Chem Phys 1983; 79(6): 2541-58.

[13] Cosby PC. Electron-impact dissociation of nitrogen. J Chem Phys 1993; 98(12): 9544.

[14] Lewis BR, Gibson ST, Zhang W, Lefebvre-Brion H, Robbe J-M. Predissociation mechanism for the lowest $^1\Pi_u$ states of N_2. J Chem Phys 2005; 122(14): 144302.

[15] Spelsberg D, Meyer W. Dipole-allowed excited states of N_2: Potential energy curves, vibrational analysis, and absorption intensities. J Chem Phys 2001;115(14): 6438-49.

[16] Khakoo MA, Malone CP, Johnson PV, *et al*. Electron-impact excitation of $X^1\Sigma_g^+$ ($v^{''}$=0) to the a'' $^1\Sigma_g^+$, $b^1\Pi_u$, $c_3^1\Pi_u$, $o_3^1\Pi_u$, b' $^1\Sigma_u^+$, c_4' $^1\Sigma_u^+$, $G^3\Pi_u$ and $F^3\Pi_u$ states of molecular nitrogen. Phys Rev A 2008; 77(1): 012704.

[17] Malone CP, Johnson PV, Liu X, Ajdari B, Kanik I, Khakoo MA. Integral cross sections for the electron-impact excitation of the $b^1\Pi_u$, $c_3^1\Pi_u$, o_3 $^1\Pi_u$, $b^{'}$ $^1\Sigma_u^+$, $c_4^{'}$ $^1\Sigma_u^+$, G $^3\Pi_u$, and $F^3\Pi_u$ states of N_2. Phys Rev A 2012; 85(6): 062704.

[18] Little DA, Tennyson J. An *ab initio* study of singlet and triplet Rydberg states of N_2. J Phys B 2013; 46: 145102.

[19] Capitelli M, Celiberto R. Electron-molecule cross sections for plasma applications: the role of internal energy of the target. In: Becker KH, Ed. Novel Aspects of Electron-Molecule Collisions 1998; p. 283.

[20] Lewis BR, Banerjee SS, Gibson ST. Asymmetric line shapes in the indirect predissociation of the $f^1\Sigma_u^+$ Rydberg state of O_2. J Chem Phys 1995; 102(17): 6631-40.

[21] Abrashkevich AG, Abrashkevich DG. FDEXTR 2.1: A new version of a program for the finite-difference solution of the coupled-channel Schrödinger equation using the Richardson extrapolation. Comp Phys Commun 1998; 113(1): 105-7.

[22] Adamson S, Astapenko V, Deminskii M, *et al*. Electron impact excitation of molecules: Calculation of the cross section using the similarity function method and ab initio data for electronic structure. Chem Phys Lett 2007; 436: 308-13.

[23] Gibson ST, Lewis BR. Understanding diatomic photodissociation with a coupled-channel Schrödinger equation model. J Electron Spectros Relat Phenomena 1996; 80: 9-12.

[24] Zipf EC, Gorman MR. Electron-impact excitation of the singlet states of N_2. I. The Birge-Hopfield system ($b^1\Pi_u$ - $X^1\Sigma_g^+$). J Chem Phys 1980; 73(2): 813-9.

[25] Morrison MA, Lane NF, Collins LA. Low-energy electron-molecule scattering: Application of coupled-channel theory to e-CO_2 collisions. Phys Rev A 1977;15(6): 2186-201.

[26] Cadez I, Gresteau F, Tronc M, Hall RI. Resonant electron impact excitation of CO_2 in the 4 eV region. J Phys B 1977; 10(18): 3821.

[27] McCurdy CW, Isaacs WA, Meyer H-D, Rescigno TN. Resonant vibrational excitation of CO_2 by electron impact: Nuclear dynamics on the coupled components of the $^2\Pi_u$ resonance. Phys Rev A 2003; 67: 042708.

[28] Allan M. Selectivity in the excitation of fermi-coupled vibrations in CO_2 by impact of slow electrons. Phys Rev Lett 2001; 87(3): 033201.

[29] Morgan LA. Virtual states and resonances in electron scattering by CO_2. Phys Rev Lett 1998; 80(9):1873-5.

[30] Tennyson J, Morgan LA. Electron collisions with polyatomic molecules using the R-matrix method. Philos Trans A 1999; 357(1755):1161-73.

[31] Mazevet S, Morrison MA, Morgan LA, Nesbet RK. Virtual-state effects on elastic scattering and vibrational excitation of CO_2 by electron impact. Phys Rev A 2001; 64: 040701.

[32] Allan M. Vibrational structures in electron-CO_2 scattering below the $^2\Pi_u$ shape resonance. J Phys B 2002; 35(17): L387.

[33] Itikawa Y. Cross sections for electron collisions with carbon dioxide. J Phys Chem Ref Data 2002; 31(3): 749-67.

[34] Rescigno TN, Isaacs WA, Orel AE, Meyer H-D, McCurdy CW. Theoretical study of resonant vibrational excitation of CO_2 by electron impact. Phys Rev A 2002; 65(3): 032716.

[35] Werner HJ, Knowles PJ, Knizia G, *et al*. MOLPRO, version 2010.1, a package of ab initio programs. Available from: http://www.molpro.net.

[36] Tennyson J. Electron-molecule collision calculations using the R-matrix method. Phys Rep 2010; 491(2-3): 29-76.

[37] Carr JM, Galiatsatos PG, Gorfinkiel JD, *et al*. UKRmol: a low-energy electron- and positron-molecule scattering suite. Eur Phys J D 2012; 66: 58.

[38] Tennyson J, Noble CJ. RESON: A program for the automatic detection and fitting of Breit-Wigner resonances. Comput Phys Commun 1984; 33(4): 421-4.

[39] Comer J, Read FH. Electron impact studies of a resonant state of N_2^-. J Phys B 1971; 4(8): 1055.

[40] Wadehra JM, Bardsley JN. Vibrational- and rotational-state dependence of dissociative attachment in e-H_2 Collisions. Phys Rev Lett 1978; 41(26): 1795-8.

[41] Bardsley JN, Wadehra JM. Dissociative attachment and vibrational excitation in low-energy collisions of electrons with H_2 and D_2. Phys Rev A 1979; 20(4): 1398-405.

[42] Atems DE, Wadehra JM. Resonant contributions to dissociation of H_2 by low-energy electron impact. J Phys B 1993; 26(21): L759.

[43] Horáček J, Čížek M, Houfek K, Kolorenč P, Domcke W. Dissociative electron attachment and vibrational excitation of H_2 by low-energy electrons: Calculations based on an improved nonlocal resonance model. II. Vibrational excitation. Phys Rev A 2006; 73(2): 022701.

[44] Horáček J, Čížek M, Houfek K, Kolorenč P, Domcke W. Dissociative electron attachment and vibrational excitation of H_2 by low-energy electrons: Calculations based on an improved nonlocal resonance model. Phys Rev A 2004; 70(5): 052712.

[45] Wadehra JM. Rates of dissociative attachment of electrons to excited H_2 and D_2. Appl Phys Lett 1979; 35(12): 917-9.

[46] Stibbe DT, Tennyson J. Near-threshold electron impact dissociation of H_2. N J Phys 1998; 1: 2.

[47] Stibbe DT, Tennyson J. Rates for the electron impact dissociation of molecular hydrogen. Astrophys J Lett 1999; 513(2): L147-L150.

[48] Trevisan CS, Tennyson J. Calculated rates for the electron impact dissociation of molecular hydrogen, deuterium and tritium. Plasma Phys Control Fusion 2002; 44(7): 1263-76.

[49] Celiberto R, Janev RK, Laporta V, Tennyson J, Wadehra JM. Electron-impact vibrational excitation of vibrationally excited H_2 molecules involving the resonant $^2\Sigma_g^+$ Rydberg-excited electronic state. Phys Rev A 2013; A(88): 062701.

Received: May 6, 2013 Revised: October 7, 2013 Accepted: December 9, 2013